CHEMISTRY
A EUROPEAN JOURNAL

DOI: 10.1002/chem.200600523

The Nature of Halogen···Halogen Synthons: Crystallographic and Theoretical Studies

Firas F. Awwadi,*[a] Roger D. Willett,[c] Kirk A. Peterson,[c] and Brendan Twamley[b]

Abstract: A study of the halogen···halogen contacts in organic compounds using ab initio calculations and the results of previously reported crystallographic studies show that these interactions are controlled by electrostatics. These contacts can be represented by the geometric parameters of the C–X_1···X_2–C moieties (where θ_1 = C–X_1···X_2 and θ_2 = X_1···X_2–C; r_i = X_1···X_2 distance). The distributions of the contacts within the sum of van der Waals radii (r_{vdW}) versus θ_i ($\theta_1 = \theta_2$) show a maximum at $\theta \approx 150°$ for X = Cl, Br, and I. This maximum is not seen in the distribution of F···F contacts. These results are in good agreement with our ab initio calculations. The theoretical results show that the position of the maximum depends on three factors: 1) The type of halogen atom, 2) the hybridization of the *ipso* carbon atom, and 3) the nature of the other atoms that are bonded to the *ipso* carbon atom apart from the halogen atom. Calculations show that the strength of these contacts decreases in the following order: I···I > Br···Br > Cl···Cl. Their relative strengths decrease as a function of the hybridization of the *ipso* carbon atom in the following order: $sp^2 > sp > sp^3$. Attaching an electronegative atom to the carbon atom strengthens the halogen···halogen contacts. An electrostatic model is proposed based on two assumptions: 1) The presence of a positive electrostatic end cap on the halogen atom (except for fluorine) and 2) the electronic charge is anisotropically distributed around the halogen atom.

Keywords: ab initio calculations · crystal engineering · halogens · intermolecular interactions

Introduction

Intermolecular interactions are of particular significance in chemistry, mainly because these interactions are responsible for stabilizing many important molecules, for example, DNA and proteins.[1a] They are also responsible for the arrangement of molecular species in crystalline lattices. Hence, they are one of the main foci of crystal engineering.[1] As well as their structural role, intermolecular interactions affect the physical properties of crystalline materials, for example, nonlinear optical properties, electrical, and magnetic properties.[2a] Intermolecular interactions are also involved in arranging reactants for pericyclic solid-state chemical reactions, cycloaddition reactions, and solid-state polymerization reactions.[1d,2b–d] The classical hydrogen bond, an example of a strong intermolecular force, has been widely studied over many years and is utilized in crystal engineering as a structural member.[1,3] More recently, other weaker interactions, for example, halogen bonds,[4] nonclassical hydrogen bonds,[5] halogen···halogen interactions,[6] and π–π stacking, have been examined with a view to utilization in crystal engineering.[7]

Halogen···halogen (R–X_1···X_2–R) contacts are characterized by an interhalogen distance (r_i) that is less than the sum of the van der Waals radii (r_{vdW}). Studies have shown that there are two preferred geometries for halogen···halogen contacts (Scheme 1). The first arrangement occurs when $\theta_1 = \theta_2$, (where θ_1 and θ_2 are the R–X_1···X_2 and X_1···X_2–R angles, respectively). The second geometry arises when $\theta_1 \approx 180°$ and $\theta_2 \approx 90°$; the perpendicular arrangement (Scheme 1).[6] This knowledge has been used to develop new

[a] Dr. F. F. Awwadi
Department of Chemistry
Jordan University of Science and Technology
Irbid (Jordan)
Fax: (+1) 509 335 8867
E-mail: fawwadi@yahoo.com

[b] Dr. B. Twamley
University Research Office, University of Idaho
Moscow, ID 83844 (USA)

[c] Prof. R. D. Willett, Prof. K. A. Peterson
Department of Chemistry, Washington State University
Pullman, WA 99164 (USA)

Supporting information (table of interaction parameters in halobenzene structures; table of interaction energies and distances for various basis sets) for this article is available on the WWW under http://www.chemeurj.org/ or from the author.

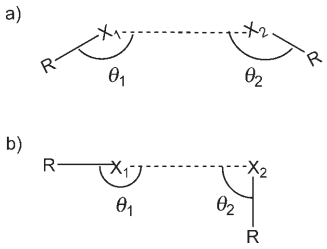

Scheme 1. The two preferred geometries for halogen···halogen contacts: a) $\theta_1=\theta_2$ and b) $\theta_1=180°$, $\theta_2=90°$. (R = organic group, X = Cl, Br, and I.)

materials and to explain the structural behavior of other important materials.[8] One example is the use of chlorine···chlorine interactions to prepare highly stereoregular organic polymers.[2b]

Chlorine···chlorine interactions have been a matter of interest and debate in recent years. Some research groups consider chlorine···chlorine interactions to be a result of attractive interactions.[6,9,10] Initially, the interaction was considered an example of a donor–acceptor interaction.[9] Another study showed that electrophiles tend to approach the halogen atom of the C–X bond (X = Cl, Br, or I) at an angle of around 100°, while nucleophiles approach the halogen atom at an angle of around 165°.[8] These results were explained in terms of charge transfer from the HOMO of the donor to the LUMO of the acceptor.[10] More recently, Desiraju and co-workers, based on a statistical analysis of the crystal structure of halogenated hydrocarbons, found that the number of contacts between the halogen atoms (Cl, Br, and I only) is greater than the number of contacts expected from the exposed area of the halogen atom alone, which is evidence for the presence of attractive forces between the two atoms involved in the halogen···halogen contact.[6a] Studies by Price et al. and Nyberg and Wong-Ng using theoretical ab initio quantum mechanical calculations and crystal structure analysis of chlorinated organic compounds indicated that Cl···Cl contacts are just a result of the packing of anisotropic atoms inside the crystals and the directionality, if any, is due only to the reduction of the exchange repulsion forces rather than to attractive forces.[11]

Crystallographic studies that have tackled this issue have not distinguished between the hybridization of the carbon atom bonded to the halogen atom and the nature of the other atoms that are attached to the carbon atom. These differences are expected to have a major effect on the halogen···halogen interaction. In this research, to resolve the dilemma of the exact physical nature of halogen···halogen contacts, crystallographic population analysis and theoretical studies were carried out. These studies show that the intermolecular contacts are mainly controlled by electrostatics.

Methods

Crystallographic study: The Cambridge Structural Database (CSD), version 5.25 November 2003, was searched for halogen···halogen (F, Cl, Br, and I) intermolecular contacts within the sum of the van der Waals radii in room-temperature structures[12] (eight filters were applied to the search: only organic compounds,[13] a crystallographic R factor <0.075, no errors in the crystal structures, no ions, not disordered, not polymeric, three-dimensional coordinates determined, no powder structures). Structures with the lowest R value were selected for analysis from multiple repeat structures. Details of each search are listed in Table 1.

Table 1. Number of halogen···halogen contacts within the sum of the van der Waals radii in the CSD.

Interaction type	No. of contacts	No. of contacts $\theta_1=\theta_2$	No. of contacts $\theta_1=\theta_2$, $\theta>90°$	No. of contacts[a] $\theta_1=\theta_2$, $\theta>90°$ $170°<\Phi<190°$	Hybridization
F···F	324	81	81	70	sp^3
	317	77	69	58	sp^2
	219	67	59	50	aromatic
Cl···Cl	323	135	132	121	sp^3
	560	216	209	198	sp^2
	378	148	142	138	aromatic
Br···Br	161	65	65	58	sp^3
	219	85	82	73	sp^2
	158	61	60	55	aromatic
I···I	23	11	11	11	sp^3
	68	17	15	13	sp^2
	40	14	13	9	aromatic

[a] Φ = C–X_1···X_2–C torsion angle.

The contacts were sorted into two categories: 1) $\theta_1=\theta_2$ and 2) $\theta_1\neq\theta_2$. We concentrated on the former interaction because other factors, such as steric hindrance and interactions with the rest of the molecule, can play a dominant role in the latter category. For X = Cl and Br, approximately 40% of the contacts fall into the $\theta_1=\theta_2$ category, with somewhat less doing so for X = F and I. To make this statistical analysis correlate with our calculations, those contacts with torsion angles Φ(C–X_1···X_2–C) (Scheme 2) between 170 and 190° were the only ones used in the statistical analysis. These represent approximately 90% of the above contacts. Contacts with $\theta_i<90°$ were ignored since at these values, other types of interaction are expected to play a dominant role.

Theoretical study: Gaussian 98 and Gaussian 03[14] were used for geometry optimization and MOLPRO[15] was used for the electronic energy calculations. The structures of the molecular units of each model were optimized by using Møller–Plesset second-order perturbation theory (MP2) with a triple-zeta basis set. The total electronic energies were computed

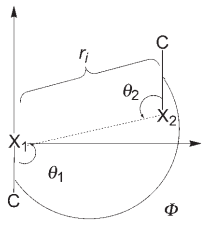

Scheme 2. Parameters used for the modeling of the halogen···halogen contacts.

by using the cc-pVnZ basis set on carbon and hydrogen atoms, aug-cc-pVnZ on bromine, chlorine, and fluorine atoms, and aug-cc-pVnZ-PP on the iodine atom with MP2 theory (n = D, T, and Q for double, triple, and quadruple zeta, respectively; aug denotes the presence of a diffuse function on the halogen atoms).[16] This approach initially involves the use of Hartree–Fock self-consistent field calculations to determine the molecular orbitals and then subsequent MP2 calculations to determine the electron correlation energy. The calculated energies of interaction were corrected for basis set superposition errors (BSSE) in models **1** and **3** (Scheme 3) using the counterpoise method.[17] With a complete basis set,

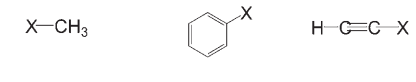

1a : X = F	**2a** : X = F	**3a** : X = F
1b : X = Cl	**2b** : X = Cl	**3b** : X = Cl
1c : X = Br	**2c** : X = Br	**3c** : X = Br
1d : X = I	**2d** : X = I	**3d** : X = I

Scheme 3. Structures of the modeled compounds **1**–**3**.

the corrected and uncorrected energy values are expected to converge. The minimum energies of interaction determined using a complete basis set E(cbs) were estimated using Equation (1), where $n = 2$, 3, or 4 and is the cardinal number of the correlation consistent basis set, and A and B are are adjustable parameters.[18]

$$E(n) = E(\mathrm{cbs}) - A\mathrm{e}^{-(n-1)} - B\mathrm{e}^{-(n-1)^2}$$

Halomethane (**1**), halobenzene (**2**), and haloaceteylene (**3**) molecules were used to model contacts of the types 1) Csp^3–X···X–Csp^3, 2) Csp^2–X···X–Csp^2, and 3) Csp–X···X–Csp, respectively (Scheme 3). The interactions were modeled by calculating the energy of interaction of two monomers as a function of the separation distance r_1 and the angle θ_i ($\theta_i = \theta_1 = \theta_2$, Scheme 2), with θ_i increased from 80 to 180° in increments of 10° with a torsion angle (Φ) of 180° (Scheme 2). The energies of interaction for the molecules **2** were modeled for two different geometries: 1) All the atoms of the dimers of **2** located in the mirror plane and 2) the mirror plane contains the two halogen atoms and is perpendicular to the planes of the phenyl rings (Scheme 4).

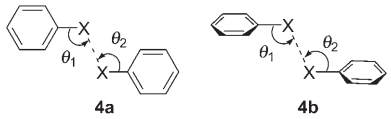

Scheme 4. A schematic representation of the two different geometries used for the models of the halogen···halogen contacts in an aromatic dimer.

Results

Crystallographic study: Investigation of the CSD shows that the maximum number of reported contacts occurs for Cl···Cl interactions with the amount of interactions decreasing in the order F > Br ≫ I. The histogram distribution for the number of contacts within the sum of the van der Waals radii versus the interaction angle θ_i ($\theta_i = \theta_1 = \theta_2$, $\theta_i > 90°$, Φ = 170–190°) shows that the maximum number of contacts occurs between 140 and 160° (Figure 1) for all interactions except F···F. From the data there are no statistically significant trends in F···F contacts. Henceforth, F···F contacts will be omitted from our discussion in this section. The interaction angle maxima vary according to the halogen (Cl···Cl, 150–160°; Br···Br, 140–150°; I···I, 145–155°). Closer examination of the data shows definite trends in hybridization effects.

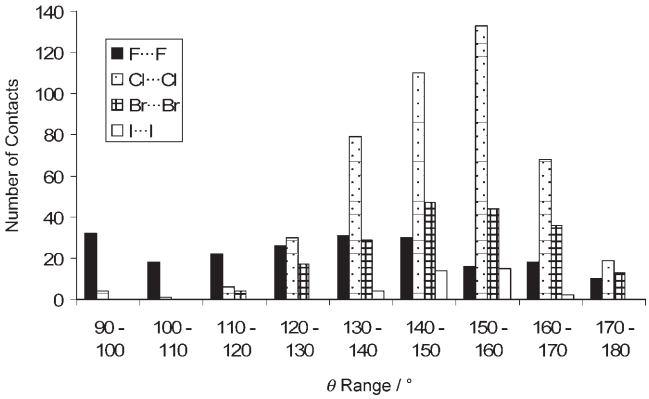

Figure 1. Histogram distribution for the number of contacts within the sum of r_{vdW} versus the interaction angle for all halogen contacts with $\theta_i = \theta_1 = \theta_2$, $\theta_i > 90$, Φ = 170–190°.

Hybridization effects: The data were sorted according to the *ipso*-carbon hybridization (Table 1). Individual histograms are shown in Figure 2 for a) Csp^3–X···X–Csp^3, b) Csp^2–X···X–Csp^2, and c) Carom–X···X–Carom (X = Cl, Br, and I) interactions. The subset (c) was treated as a special case separate from (b). Experimentally, they display distinct and different trends. The interaction angle maximum depends on both the hybridization and the type of halogen atom. The dependence of the maxima on hybridization decreases in the order Csp^3–X···X–Csp^3 > Csp^2–X···X–Csp^2 > Carom–X···X–Carom. From Figure 2c it is clear that the aromatic cases have the maximum shifted to between 140 and 150°, which compares with the maximum for all the sp^2-hybridized cases (both aromatic and aliphatic) of around 150–160°. The data for the number of Cl···Cl contacts in the maximum ranges of 150–160° (Csp^3–Cl, Csp^2–Cl) and 140–150° (Carom–Cl) as a function of separation distance in 0.05 Å increments display discrete maxima (Figure 3). These maxima indicate that the most frequent separation distances for the Csp^3–Cl, Csp^2–Cl, and Carom–Cl dimer species are 0.08, 0.18, and 0.03 Å shorter than the sum of the van der Waals radii, respectively. The number of contacts for the other halogen···halogen contacts is not large enough to perform such a statistical analysis.

Theoretical study: Three basis sets of increasing size were used to model the halogen···halogen contacts in the model compounds **1a** to **3d** (see Scheme 3). The energies of interaction were also estimated at the complete basis set (CBS) level. In addition, the energies of interaction for the dimers of **1** and **3** were corrected for basis set superposition error (BSSE). For dimers of **2**, this correction was not possible with the computer resources available. However, at the CBS level, this correction was estimated to be less than

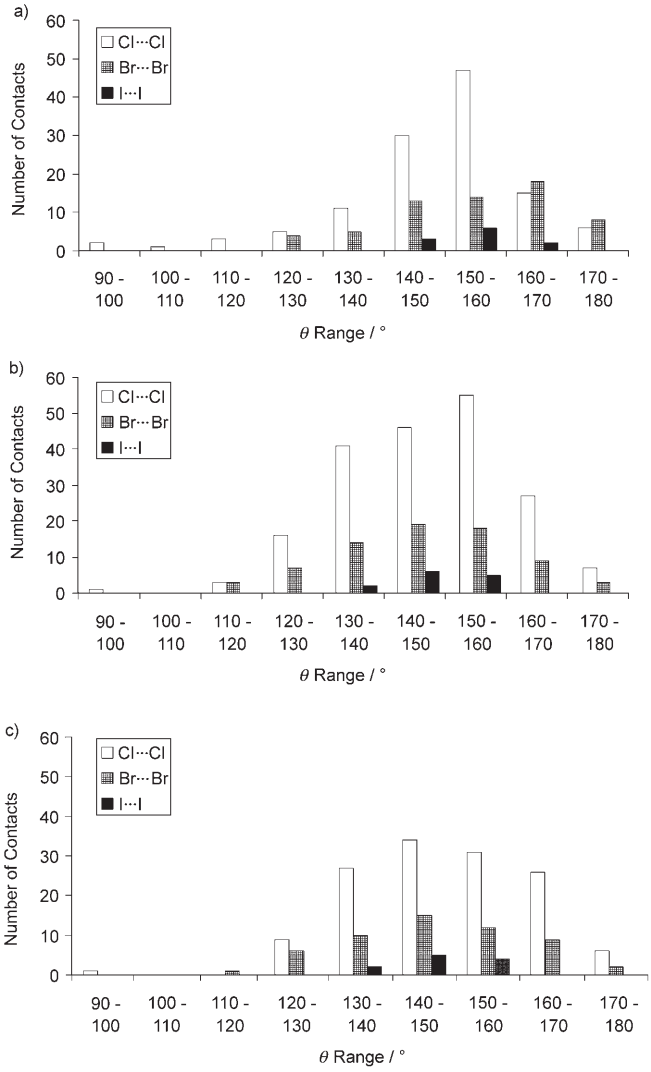

Figure 2. Histogram of the number of contacts within the sum of r_{vdW} for molecules of the type a) Csp^3–X···X–Csp^3, b) Csp^2–X···X–Csp^2, and c) Carom–X···X–Carom.

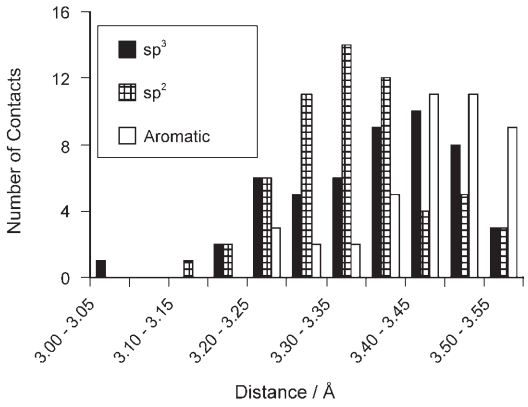

Figure 3. Histogram of the number of contacts as function of the chlorine···chlorine separation distances.

the basis set level decreases the separation distance to within the sum of the van der Waals radii (for the ≈150° geometry). The energies of interaction calculated at the ≈150° minimum decrease in the order I···I > Br···Br > Cl···Cl (Table 2). The stabilization energies were calculated as a function of the hybridization of the *ipso* carbon. The stabilization energies decrease in the order $sp^2 > sp > sp^3$. The effects of hybridization of the *ipso* carbon atom in the halogen···halogen contacts are outlined in the following sections.

Csp^3–X···X–Csp^3 contacts: The potential-energy diagrams for two interacting monomers of molecule **1** were calculated at the double-zeta basis set level for $\theta_1 = \theta_2$ geometries and both angles were varied from 80 to 180°. The contour plot for type **1a** dimers shows only one minimum at $\theta < 80°$ (Figure 4a). Plots for **1b**, **1c**, and **1d** show two minima; the first one at around 150° (Figure 4b), the second again at angles less than 80°. At both minima, the calculated separation distances are larger than the sum of the van der Waals radii. Significantly, the use of larger basis sets, up to and including an estimation of the results for the complete basis set, 0.5 kJ mol^{-1}. The potential-energy diagrams calculated at the double-zeta (dz) basis set level (see the Methods section) indicate an energy minimum at ≈150° ($\theta_1 = \theta_2$, $\Phi = 180°$) for all of the model compounds except those containing fluorine (Figure 4). The energies of interaction at this value of θ, as a function of r_i, were calculated by using triple- (tz) and quadruple-zeta (qz) basis sets. At the double-zeta level, all energy minima occur at distances larger than the sum of the van der Waals radii. Increasing

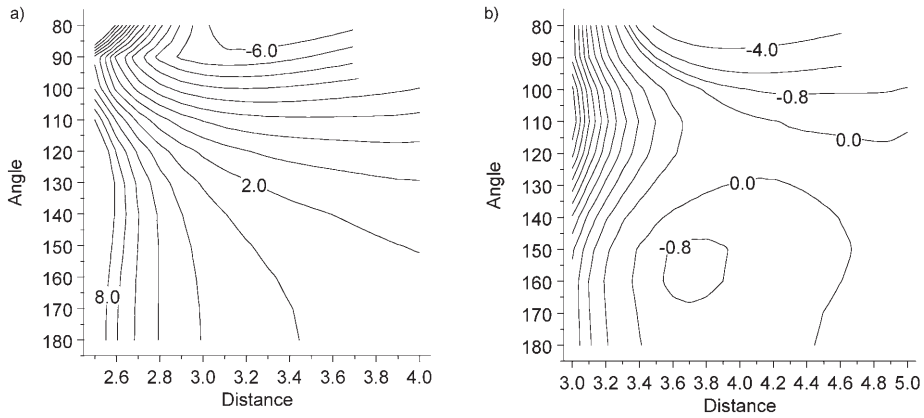

Figure 4. Potential-energy diagrams at the MP2/dz level of theory for two interacting molecules **1** as a function of the angle θ_i and distance r_i for a) **1a** and b) **1b** with $\theta_2 = \theta_1$. Molecules **1c** and **1d** exhibit similar plots to that of **1b**. The separation distances, energies, and angles are listed in Table 2.

Table 2. Calculated energies of interaction, separation distances, and angles of interaction for the energy minima at ≈150° (Figure 4b) for the model compounds computed at the double-zeta and complete basis set levels.[a]

	Double-zeta basis set			Complete basis set		
	angle [°]	distance [Å]	energy [kJ mol^{-1}]	angle [°]	distance [Å]	energy [kJ mol^{-1}]
			dimers of molecules **1**			
1b	156	3.71	−1.027	156	3.43	−2.770
1c	153	3.82	−2.484	153	3.60	−4.826
1c[b]	153	3.68	−4.373	153	3.58	−5.207
1d	147	4.15	−4.260	147	3.86	−7.585
			dimers of molecules **2**[c]			
2b	152	3.46	−5.502	152	3.38	−5.216
2c	150	3.72	−6.180	150	3.65	−8.766
2d	148	3.96	−8.430	148	3.81	−9.029
			dimers of molecules **3**			
3b	142	3.66	−2.731	142	3.46	−4.129
3c	140	3.85	−3.552	140	3.65	−5.425
3d	144	4.11	−3.745	144	4.04	−6.073

[a] See Table 2S in the Supporting Information for results of the triple- and quadruple-zeta basis set calculations. [b] Values not corrected for BSSE errors are included for comparison purposes. [c] The energies for the dimers of molecules **2** are not corrected for BSSE errors.

moves the calculated energy minimum to within the sum of the van der Waals radii (see Table 2).

Csp^2–X···X–Csp^2 contacts: Energy minima at around 150° are seen when $\theta_1=\theta_2$ and $\Phi=180°$ for all of the halogen···· halogen contacts (except F···F). These minima are shifted to lower angles in comparison with the Csp^3–X···X–Csp^3 contacts. With all of the atoms lying in the mirror plane, the other minimum is located at around 90°. Conversely, when the mirror plane bisects the aromatic system, the minimum occurs at $\theta<80°$. At these smaller angles, the positions of this minimum are affected by other interactions, that is, C–H···X hydrogen bonds, interaction with the aromatic system, and steric repulsion.

Csp–X···X–Csp contacts: Relative to the interactions in compounds **1** and **2**, compounds **3** have an energy minimum that is shifted to lower angles, with an increase in the separation distance (Table 2).

Discussion

Both the crystallographic and the theoretical data will be discussed in the following order: 1) Proposal of the model, 2) the effect of hybridization of the *ipso* carbon atom and its influence on the separation distance between the two halogen atoms and the most suitable geometry, 3) comparison of this model with simple crystal structures, and 4) the effect of attaching an electronegative atom to the *ipso* carbon atom.

Model: An electrostatic model can be used to explain the theoretical and crystallographic data. Such a model is based on two main ideas. 1) The calculated electrostatic potentials show the presence of a positive potential end cap and a negative electrostatic potential ring in the π region of the halogen atoms (except for the fluorine atom), as illustrated in Figure 5 for molecules **1**. 2) The electron density is anisotropically distributed around the halogen atom (Figure 5b). In Figure 5b, the electron density has been multiplied by a factor for all atoms to enhance the anisotropy. Thus, a quantitative comparison between molecules cannot be made.[11a,19] The data in these figures illustrate that the halogen atoms have two different radii; a shorter one along the C–X bond and a longer one perpendicular to it. According to the electrostatic model, the presence of an energy minimum dictates that the negative electrostatic ring should face the positive electrostatic end cap. In view of this, two energy minima are expected between the two halogen atoms. These minima occur for the following geometries: 1) $\theta_1=\theta_2\approx150°$ and a torsion angle (C–X···X–C) of $\Phi=180°$ (Figure 6a) and 2) $\theta_2=180$ and $\theta_1=90°$ (Figure 6b). In this discussion, the type (2) interactions will not be analyzed in detail owing to the fact that other effects (intermolecular interactions, steric, electronic, etc.) will influence these interactions. Nevertheless, the stability of this geometry is expected based on the electrostatic model. For the type (1) interactions, the

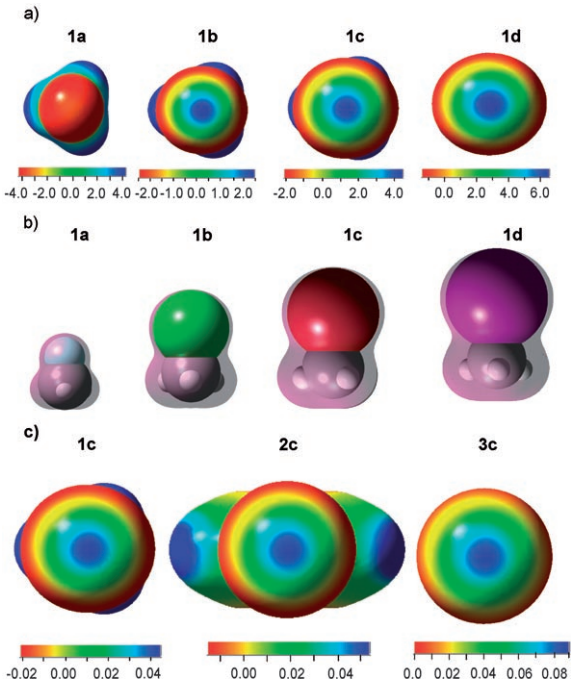

Figure 5. a) Calculated electrostatic potential surface for **1a**, **1b**, **1c**, and **1d**, respectively. b) Electron density of **1a**, **1b**, **1c**, and **1d**. The anisotropy in the electronic charge distribution is represented by the umbra around the spherical halogen; the umbra radius along the C–X bond is smaller than the radius perpendicular to it. c) The calculated electrostatic potential of **1c**, **2c**, and **3c**. The energy is expressed in hartrees and the charge in electronic charge units (the scale is multiplied by 100). The electron density contour isovalue is set to 0.005. The potential and electron density were calculated using MP2 and a tz basis set.

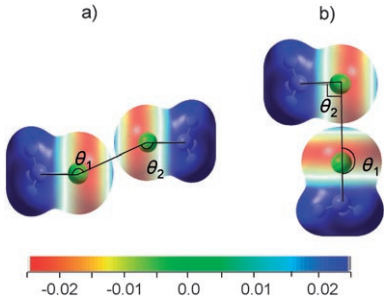

Figure 6. Geometries of the two energy minima of **1b**: a) $\theta_1=\theta_2\approx150°$, torsion angle (C–X···X–C), $\Phi=180°$; b) $\theta_2=180$ and $\theta_1=90°$. The color variation indicates the value of the calculated electrostatic potential.

number of contacts within the sum of the van der Waals radii observed in the crystallographic database analysis agrees with an electrostatic model and our ab initio calculations. The three heavier halogen atoms (Cl, Br, and I) display interaction maxima in the range of 140–160°. No minimum is observed in the area for F···F interactions, in accord with experimental observations. The calculations also indicate that as the size of the halogen atom increases the relative strengths of the halogen···halogen contacts increase. This supports the argument for the deformation of the electronic charge around the halogen atom, since the heavier halogen atoms are more polarizable.

The role of anisotropy in the van der Waals radii and the presence of the positive electrostatic potential end caps on the halogen atoms can be tested by investigating the distance at which the energy minimum is located as a function of the angle θ in type (1) interactions. Figure 7 shows that the energy minimum occurs when $150°<\theta<160°$. When $\theta=180°$, the radii of the halogen atoms are the smallest. However, electrostatic repulsion forces between the positive end caps cause the energy minima to shift to higher separation distances. However, the interaction is still attractive owing to the presence of other forces, for example, dispersion. As the angle θ approaches 150°, the separation distances at the

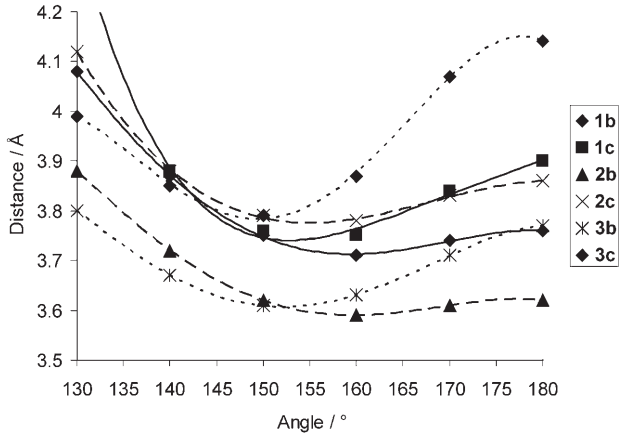

Figure 7. Plot of the angle, θ, at which the calculated energy minimum is located versus the corresponding separation distance, r_i. The drawn curves are guides for the eye only.

energy minima decrease, even though the radii are increasing. This decrease in separation distance is due to the attractive forces between the positive electrostatic end cap of one halogen atom and the negative electrostatic ring of the other (Figure 6). For $\theta<150°$, the separation distance increases again due to both the increments in the radii and to the decrease in electrostatic attractions as the negative electrostatic rings start to interact with each other. Overall, the data indicate these interactions are controlled by electrostatics.

Effect of hybridization: The strength of the halogen–halogen interactions is determined primarily by the positive electrostatic potential end cap and the negative electrostatic potential ring. The strength of the interactions increases as both the positive electrostatic potential end cap and the negative electrostatic ring increase. Figure 5c shows that the positive electrostatic potential end cap tends to increase as the s character increases and the negative electrostatic potential ring tends to decrease as the s character decreases. As a result, the strength of the interaction as a function of the hybridization of the *ipso* carbon atom decreases in the order $sp^2>sp>sp^3$.

This behavior parallels the electronegativity of the *ipso* carbon atom, since there is more s character in sp-hybridized atoms. The dimers of compounds **1** have hydrogen atoms bonded to the *ipso* carbon atoms, while the dimers of compounds **2** and **3** have additional carbon atoms bonded to the *ipso* carbon. This will change the electronegativity of the *ipso* carbon atom and, hence, the energy of interaction and the distance at which this minimum occurs. The crystallographic analysis supports this idea, as indicated by the separation distance and the angle of interaction; for example, the mean Cl···Cl separation distance is 0.08 and 0.18 Å less than the sum of the van der Waals radii for Csp^3–X···X–Csp^3 and Csp^2–X···X–Csp^2, respectively (see Figure 3).

Crystal structures of the model compounds: The structures of several of the model compounds have been reported and allow comparison between the theoretical and experimental results. The structures of the monohalomethanes, CH_3X (except for X=F, which is unknown), are based on competition between hydrogen bonding and halogen···halogen contacts.[20] Hydrogen bonding is dominant in the structure of **1b** and hence there are no Cl···Cl contacts in this example.[20a] The distance between the two closest chlorine atoms is 4.141 Å, which is well outside the sum of the van der Waals radii. In contrast, the structures of **1c** and **1d** show both halogen···halogen contacts and hydrogen bonding.[20b] The structures of **1c** and **1d** are isomorphous and form chain structures based on the halogen···halogen contacts. This agrees with calculations (see above, Table 2) that show that the Br···Br and I···I interactions are stronger than Cl···Cl interactions.

Halogen···halogen contacts play a more crucial role in the structures of compounds **2** than in the structures of compounds **1**. The shortest F···F distance in the structure of fluo-

robenzene is 4.727 Å.[21a] In the structure of **2b**, chlorine atoms are directed towards each other, even though the distance between them is slightly larger than the sum of the van der Waals radii (3.599 Å).[21b] The contact angles are $\theta_1=\theta_2=147°$, which agree well with the calculated angle of $\theta_1=\theta_2=152°$. This indicates that Cl···Cl contacts are stronger when the chlorine atom is attached to an sp^2-hybridized atom than an sp^3-hybridized carbon atom.

Effect of attaching an electronegative atom to the *ipso* carbon atom: The addition of a more electronegative atom to an *ipso* carbon atom will strengthen the halogen···halogen interaction. Calculations show that the addition of fluorine to **1b** and **1c** significantly increases the energy of interaction. In contrast, the addition of more atoms with the same electronegativity has only a slight effect (Table 3). This indicates that the addition of extra electronegative atoms onto the carbon atom increases the deformation of the electronic charge and hence the positive electrostatic potential end cap.

Table 3. The calculated energies, angles, and separation distances in fluorohalomethane dimers.[a]

Compound	Energy [kJ mol^{-1}]	Angle [°]	Distance [Å]
1b	−1.027	156	3.71
FCH_2Cl	−2.163	152	3.67
F_2CHCl	−2.271	149	3.69
F_3CCl	−2.334	143	3.71
1c	−2.484	153	3.83
FCH_2Br	−3.130	150	3.86
F_2CHBr	−3.088	146	3.89
F_3CBr	−3.095	141	3.91

[a] Calculations were carried out at the dz basis set level.

Experimentally, the situation is a bit more complicated. Examination of the structures of fluorotrichloromethane and fluorotribromomethane[22] show that the highly electronegative fluorine atoms form hetero halogen···halogen interactions (F···Cl, F···Br) rather than assisting in a stronger homo halogen···halogen interaction. However, in dichlorobenzene, the interaction distance is shorter than in **2b** (see Table 1S of the Supporting Information) when $\theta_1=\theta_2$. The addition of an extra chlorine atom to the ring reinforces the Cl···Cl contact.[21b,23a] This follows from the calculations on the fluorohalomethane molecules (see above).

Other related intermolecular interactions have been shown to be electrostatic in nature.[24] Lommerse et al., based on theoretical and crystallographic studies, showed that the C−X···E interaction (X = F, Cl, Br, or I; E = N, O, or S) was mainly due to electrostatic factors.[24a] More recently, the electron density map of the molecular aggregation between 4,4′-bipyridyl *N*,*N*′-dioxide and 1,4-diiodotetrafluorobenzene, as well as for the complex of (*E*)-1,2-di(4-pyridyl)-ethylene and 1,4-diiodotetrafluorobenzene, revealed that I···O and I···N interactions are electrostatic in nature.[24b,c] The intermolecular perturbation calculations performed by Price et al. showed there is a reduction in the electrostatic repulsion at around 150°.[11a] In several crystallographic studies it was found that halogen···halide interactions (C−X···X$^-$) prefer a linear arrangement; the negatively charged halide anion confronts the positive electrostatic potential cap on the halogen.[25] Moreover, the C−X···X−M (halogen···metal halide) synthon is again characterized by a linear C−X···X arrangement and a separation distance less than the sum of the van der Waals radii.[26] Zordan et al. have shown that the C−X···X−M contacts involve an attractive electrostatic contribution.[26e] All of these observations agree with and support our electrostatic model.

Conclusion

Both the ab initio calculations and the histogram distributions of halogen···halogen contacts indicate that they are directive and a result of attractive forces for all halogens (except fluorine). These results can be understood on the basis of an electrostatic model. The model is based on two ideas: 1) The presence of a positive electrostatic potential end cap on the halogen atom (as shown by the calculated electrostatic potential) and 2) an anisotropic distribution of the electron density around the halogen atom. The interaction strength decreases in the order I···I > Br···Br > Cl···Cl. For X = F, the F···F interactions are weak enough that other intermolecular interactions dominate. This trend in halogen···halogen interaction strength parallels the polarizability of the electronic charge around the halogen atom.

The hybridization of the *ipso* carbon atom and the addition of an electronegative atom to this atom also affect the strength of halogen···halogen interactions, their geometry, and also the separation distance. Halogen···halogen interactions are strongest when the halogen atom is attached to an sp^2-hybridized atom and weakest when attached to an sp^3-hybridized atom. Adding extra electronegative atoms to the *ipso* carbon atom can reinforce these contacts. It has also been observed that a change in interaction angle and in the anisotropy in the charge distribution will affect the interaction distance. Therefore, in order to be able to regard the separation distance as an accurate parameter of the strength of the halogen···halogen contact, the contact angles should be very similar. While our crystallographic and theoretical studies show that these synthons are controlled by electrostatic factors, other forces (for example, dispersion and charge transfer) also participate in these interactions.

Finally, our calculations have shown that the dz basis set is insufficient to model the halogen···halogen contacts accurately. At this level, the model indicates that this minimum will occur at a distance longer than the sum of the van der Waals radii. However, the interaction distances derived using the complete basis set (Table 2) are in very good agreement with the experimental data.

Understanding the nature of these interactions and how to control them systematically can help in the design and synthesis of specific supramolecular synthons for crystal engineering purposes. The addition of another simple predicta-

ble supramolecular synthon element into the arsenal of crystal engineering techniques, for example, hydrogen bonding, π–π interactions, and the halogen bond, is a fundamental and important result.

Acknowledgement

This work was supported in part by the American Chemical Society Petroleum Research Fund (ACS-PRF 34779-AC).

[1] a) G. R. Desiraju, *Nature* **2001**, *412*, 397–400; b) G. R. Desiraju, *Crystal Engineering, The Design Of Organic Solids*, Elsevier Science, Amsterdam, **1989**; c) R. G. Desiraju, *Angew. Chem.* **1995**, *107*, 2541–2558; *Angew. Chem. Int. Ed. Engl.* **1995**, *34*, 2311–2327; d) L. Brammer, *Chem. Soc. Rev.* **2004**, *33*, 476–489; e) D. Braga, L. Brammer, N. Champness, *CrystEngComm* **2005**, *7*, 1–19; f) P. Metrangolo, G. Resnati, *Chem. Eur. J.* **2001**, *7*, 2511–2519.

[2] a) H. M. Yamamoto, J. Yamaura, R. Kato, *J. Am. Chem. Soc.* **1998**, *120*, 5905–5913, and references therein; b) A. Matsumoto, T. Tanaka, T. Tsubouchi, K. Tashiro, S. Saragai, Sh. Nakamoto, *J. Am. Chem. Soc.* **2002**, *124*, 8891–8902; c) L. R. MacGillivray, J. L. Reid, J. A. Ripmeester, *J. Am. Chem. Soc.* **2000**, *122*, 7817–7818; d) L. R. MacGillivray, *CrystEngComm* **2002**, *4*, 37–41.

[3] a) C. B. Aakeröy, A. M. Beatty, *Aust. J. Chem.* **2001**, *54*, 409–421; b) L. Brammer, E. A. Bruton, P. Sherwood, *Cryst. Growth Des.* **2001**, *1*, 277–290; c) H. D. Lutz, *J. Mol. Struct.* **2003**, *646*, 227–236.

[4] a) R. B. Walsh, C. W. Padgett, P. Metrangolo, G. Resnati, T. W. Hanks, W. T. Pennington, *Cryst. Growth Des.* **2001**, *1*, 165–175; b) C. Ouvrard, J. Questel, M. Berthelot, C. Laurence, *Acta Crystallogr., Sect. B* **2003**, *59*, 512–526; c) A. Forni, P. Metrangolo, T. Pilati, G. Resanti, *Cryst. Growth Des.* **2004**, *4*, 291–295; d) S. Berski, Z. Ciunik, K. Drabent, Z. Latajka, J. Panek, *J. Phys. Chem. B* **2004**, *108*, 12327–12332; e) A. Santis, A. Forni, R. Liantonio, P. Metrangolo, T. Pilati, G. Resnati, *Chem. Eur. J.* **2003**, *9*, 3974–3983; f) W. Wang, N. Wong, W. Zheng, A. Tian, *J. Phys. Chem. A* **2004**, *108*, 1799–1805; g) P. Auffinger, F. A. Hays, E. Westhof, P. Shing Ho, *Proc. Natl. Acad. Sci. USA* **2004**, *48*, 16789–16794; h) P. Metrangolo, H. Neukirch, T. Pilati, G. Resnati, *Acc. Chem. Res.* **2005**, *38*, 386–395.

[5] a) D. Braga, F. Grepioni, *New J. Chem.* **1998**, *22*, 1159–1161; b) G. R. Desiraju, T. Stiener, *The Weak Hydrogen Bond in Structural Chemistry and Biology*, Oxford University Press, Oxford, **1990**; c) P. J. Langley, J. Hulliger, R. Thaimattam, G. R. Desiraju, *New J. Chem.* **1998**, *22*, 1307–1309.

[6] a) G. R. Desiraju, R. Parthasarathy, *J. Am. Chem. Soc.* **1989**, *111*, 8725–8726; b) A. R. Jagarlapudi, P. Sarma, G. R. Desiraju, *Acc. Chem. Res.* **1986**, *19*, 222–228; c) C. M. Reddy, M. T. Kirchner, R. V. Gundakaram, K. A. Padmanabhan, G. R. Desiraju, *Chem. Eur. J.* **2006**, *12*, 2222–2234.

[7] a) M. O. Sinnokrot, D. C. Sherrill, *J. Am. Chem. Soc.* **2004**, *126*, 7690–7697; b) M. O. Sinnokrot, D. C. Sherrill, *J. Phys. Chem.* **2003**, *107*, 8377–8379; c) M. O. Sinnokrot, E. F. Valeev, D. C. Sherrill, *J. Am. Chem. Soc.* **2002**, *124*, 10887–10893; d) C. A. Hunter, K. M. Sanders, *J. Am. Chem. Soc.* **1990**, *112*, 5525–5534; e) G. R. Desiraju, A. Gavezzotti, *J. Chem. Soc., Chem. Commun.* **1989**, 621–623.

[8] a) E. Bosch, C. L. Barnes, *Cryst. Growth Des.* **2002**, *2*, 299–302; b) C. K. Broder, A. J. Howard, C. C. Wilson, F. H. Allen, R. K. Jetti, A. Nangia, G. R. Desiraju, *Acta. Crystallogr., Sect. B* **2000**, *56*, 1080–1084.

[9] A. H. Bent, *Chem. Rev.* **1968**, *68*, 587–648.

[10] N. Ramasubbu, R. Parthasarathy, P. Murray-Rust, *J. Am. Chem. Soc.* **1986**, *108*, 4308–4314.

[11] a) S. L. Price, A. J. Stone, J. Lucas, R. S. Rowland, A. E. Thornley, *J. Am. Chem. Soc.* **1994**, *116*, 4910–4918; b) S. C. Nyburg, W. Wong-Ng, *Proc. R. Soc. London, Ser. A* **1979**, *367*, 29–45.

[12] Any structure determined in the range 283–303 K is considered to be a room-temperature structure.

[13] Selecting this filter eliminates from the search any structure that contains a transition metal, lanthanide, actinide or any of Al, Ga, In, Tl, Ge, Sn, Pb, Sb, Bi, or Po.

[14] a) Gaussian 98 (Revision A.11.2), M. J. Frisch, G. W. Trucks, H. B. Schlegel, G. E. Scuseria, M. A. Robb, J. R. Cheeseman, V. G. Zakrzewski, J. A. Montgomery, Jr., R. E. Stratmann, J. C. Burant, S. Dapprich, J. M. Millam, A. D. Daniels, K. N. Kudin, M. C. Strain, O. Farkas, J. Tomasi, V. Barone, M. Cossi, R. Cammi, B. Mennucci, C. Pomelli, C. Adamo, S. Clifford, J. Ochterski, G. A. Petersson, P. Y. Ayala, Q. Cui, K. Morokuma, P. Salvador, J. J. Dannenberg, D. K. Malick, A. D. Rabuck, K. Raghavachari, J. B. Foresman, J. Cioslowski, J. V. Ortiz, A. G. Baboul, B. B. Stefanov, G. Liu, A. Liashenko, P. Piskorz, I. Komaromi, R. Gomperts, R. L. Martin, D. J. Fox, T. Keith, M. A. Al-Laham, C. Y. Peng, A. Nanayakkara, M. Challacombe, P. M. W. Gill, B. Johnson, W. Chen, M. W. Wong, J. L. Andres, C. Gonzalez, M. Head-Gordon, E. S. Replogle, J. A. Pople, Gaussian, Inc., Pittsburgh PA, **2001**; b) Gaussian 03, Revision C.02, M. J. Frisch, G. W. Trucks, H. B. Schlegel, G. E. Scuseria, M. A. Robb, J. R. Cheeseman, J. A. Montgomery, Jr., T. Vreven, K. N. Kudin, J. C. Burant, J. M. Millam, S. S. Iyengar, J. Tomasi, V. Barone, B. Mennucci, M. Cossi, G. Scalmani, N. Rega, G. A. Petersson, H. Nakatsuji, M. Hada, M. Ehara, K. Toyota, R. Fukuda, J. Hasegawa, M. Ishida, T. Nakajima, Y. Honda, O. Kitao, H. Nakai, M. Klene, X. Li, J. E. Knox, H. P. Hratchian, J. B. Cross, C. Adamo, J. Jaramillo, R. Gomperts, R. E. Stratmann, O. Yazyev, A. J. Austin, R. Cammi, C. Pomelli, J. W. Ochterski, P. Y. Ayala, K. Morokuma, G. A. Voth, P. Salvador, J. J. Dannenberg, V. G. Zakrzewski, S. Dapprich, A. D. Daniels, M. C. Strain, O. Farkas, D. K. Malick, A. D. Rabuck, K. Raghavachari, J. B. Foresman, J. V. Ortiz, Q. Cui, A. G. Baboul, S. Clifford, J. Cioslowski, B. B. Stefanov, G. Liu, A. Liashenko, P. Piskorz, I. Komaromi, R. L. Martin, D. J. Fox, T. Keith, M. A. Al-Laham, C. Y. Peng, A. Nanayakkara, M. Challacombe, P. M. W. Gill, B. Johnson, W. Chen, M. W. Wong, C. Gonzalez, and J. A. Pople, Gaussian, Inc., Wallingford CT, 2004.

[15] MOLPRO, H.-J. Werner, P. J. Knowles, J. Almlöf, R. D. Amos, A. Bernhardsson, A. Berning, P. Celani, D. L. Cooper, M. J. O. Deegan, A. J. Dobbyn, F. Eckert, S. T. Elbert, C. Hampel, G. Hetzer, T. Korona, R. Lindh, A. W. Lloyd, S. J. McNicholas, F. R. Manby, W. Meyer, M. E. Mura, A. Nicklass, P. Palmieri, R. M. Pitzer, P. Pulay, G. Rauhut, M. Schütz, H. Stoll, A. J. Stone, R. Tarroni, P. R. Taylor, T. Thorsteinsson, Cardiff, **2002**.

[16] a) T. H. Dunning, Jr., *J. Chem. Phys.* **1989**, *90*, 1007–1023; b) R. A. Kendall, T. H. Dunning, Jr., R. J. Harrison, *J. Chem. Phys.* **1992**, *96*, 6796–6806; c) D. E. Woon, T. H. Dunning, Jr., *J. Chem. Phys.* **1993**, *98*, 1358–1371; d) A. K. Wilson, K. A. Peterson, D. E. Woon, T. H. Dunning, Jr., *J. Chem. Phys.* **1999**, *110*, 7667–7676; e) K. A. Peterson, D. Figgen, E. Goll, H. Stoll, M. Dolg, *J. Chem. Phys.* **2003**, *119*, 11113–11123.

[17] S. F. Boys, F. Bernardi, *Mol. Phys.* **1970**, *19*, 553.

[18] a) K. A. Peterson, D. E. Woon, T. H. Dunning, Jr., *J. Chem. Phys.* **1994**, *100*, 7410–7415; b) D. Feller, K. A. Peterson, *J. Chem. Phys.* **1999**, *110*, 8384–8396.

[19] S. C. Nyburg, C. H. Faerman, *Acta Crystallogr., Sect. B* **1985**, *41*, 274–279.

[20] a) R. D. Burbank, *J. Am. Chem. Soc.* **1953**, *75*, 1211–1214; b) T. Kawaguchi, M. Hijikigawa, Y. Hayafuji, M. Ikeda, R. Fukushima, Y. Tomiie, *Bull. Chem. Soc. Jpn.* **1973**, *46*, 53–56.

[21] a) V. R. Thalladi, H.-C. Weiss, D. Blaeser, R. Boese, A. Nangia, G. R. Desiraju, *J. Am. Chem. Soc.* **1998**, *120*, 8702–8710; b) D. Andre, R. Fourme, M. Renaud, *Acta Crystallogr. Sect. B* **1971**, *27*, 2371–2380.

[22] a) J. K. Cockcroft, A. N. Z. Fitch, *Z. Kristallogr.* **1994**, *209*, 488–490; b) A. N. Fitch, J. K. Cockcroft, *Z. Kristallogr.* **1992**, *202*, 243–250.

[23] a) R. Boese, M. T. Kirchner, J. D. Duntiz, G. Filippini, A. Gavezzotti, *Helv. Chim. Acta* **2001**, *84*, 1561–1577; b) U. Croatto, S. Bezzi, E. Bua, *Acta Crystallogr.* **1952**, *5*, 825–829; c) E. Estop, A. Alvarez-Larena, A. Belaaraj, X. Solans, M. Labrador, *Acta Crystallogr., Sect.*

C **1997**, *53*, 1932–1935; d) J. Housty, J. Clastre, *Acta Crystallogr.* **1957**, *10*, 695–698; e) G. L. Wheeler, S. D. Colson, *Acta Crystallogr., Sect. B* **1975**, *31*, 911–913; f) R. Fourme, G. Clec'h, P. Figuiere, M. Ghelfenstein, H. Szwarc, *Mol. Cryst. Liq. Cryst.* **1974**, *27*, 315–323; g) G. L. Wheeler, S. D. Colson, *J. Chem. Phys.* **1976**, *65*, 1227–1235; h) C. Panattoni, E. Frasson, S. Bezzi, *Gazz. Chim. Ital.* **1963**, *93*, 813–822.

[24] a) J. P. Lommerse, A. J. Stone, R. Taylor, F. H. Allen, *J. Am. Chem. Soc.* **1996**, *118*, 3108–3116; b) R. Bianchi, A. Forni, T. Pilati, *Acta Crystallogr., Sect. B* **2004**, *60*, 559–568; c) R. Bianchi, A. Forni, T. Pilati, *Chem. Eur. J.* **2003**, *9*, 1631–1638; d) J. Zou, Y. Jiang, M. Guo, J. Hu, B. Zhang, H. Liu, Q. Yu, *Chem. Eur. J.* **2005**, *11*, 740–751.

[25] a) M. Freytag, P. G. Jones, *Z. Naturforsch. B* **2001**, *56*, 889–896; b) M. Freytag, P. G. Jones, B. Ahrens, A. K. Fischer, *New J. Chem.* **1999**, *23*, 1137–1139; c) Th. Logothetis, F. Meyer, P. Metrangolo, T. Pilati, G. Resnati, *New J. Chem.* **2004**, *28*, 760–763; d) N. Kuhn, A. Abu-Rayyan, K. Eichele, S. Schwarz, M. Steimann, *Inorg. Chim. Acta* **2004**, *357*, 1799–1804; e) N. Kuhn, N. A. Abu-Rayyan, K. Eichele, C. Piludu, M. Steimann, *Z. Anorg. Allg. Chem.* **2004**, *630*, 495–497.

[26] a) R. D. Willett, F. F. Awwadi, R. Butcher, S. Haddad, B. Twamley, *Cryst. Growth Des.* **2003**, *3*, 301–311; b) L. Brammer, G. M. Espallargas, H. Adams, *CrystEngComm* **2003**, *5*, 343–345; c) S. Haddad, F. Awwadi, R. D. Willett, *Cryst. Growth Des.* **2003**, *3*, 501–505; d) F. Zordan, L. Brammer, *Acta Crystallogr., Sect. B* **2004**, *60*, 512–519; e) F. Zordan, L. Brammer, P. Sherwood, *J. Am. Chem. Soc.* **2005**, *127*, 5979–5989.

Received: April 12, 2006
Published online: September 14, 2006

